

# High-Temperature Measurement of Seebeck Coefficient and Electrical Conductivity

J. DE BOOR,<sup>1,3</sup> C. STIEWE,<sup>1</sup> P. ZIOLKOWSKI,<sup>1</sup> T. DASGUPTA,<sup>1</sup>  
G. KARPINSKI,<sup>1</sup> E. LENZ,<sup>2</sup> F. EDLER,<sup>2</sup> and E. MUELLER<sup>1</sup>

1.—German Aerospace Center, Institute of Materials Research, Linder Höhe, 51147 Köln, Germany. 2.—Physikalisch-Technische Bundesanstalt, Abbestraße 2-12, 10587 Berlin, Germany. 3.—e-mail: johannes.deboor@dlr.de

We have developed a system for simultaneous measurement of the electrical conductivity and Seebeck coefficient for thermoelectric samples in the temperature region of 300 K to 1000 K. The system features flexibility in sample dimensions and easy sample exchange. To verify the accuracy of the setup we have referenced our system against the NIST standard reference material 3451 and other setups and can show good agreement. The developed system has been used in the search for a possible high-temperature Seebeck standard material. FeSi<sub>2</sub> emerges as a possible candidate, as this material combines properties typical of thermoelectric materials with large-scale fabrication, good spatial homogeneity, and thermal stability up to 1000 K.

**Key words:** Thermoelectrics, measurement technique, measurement of Seebeck coefficient, Seebeck coefficient reference material

## INTRODUCTION

Thermoelectricity deals with direct conversion of heat into electrical energy and can therefore make a valuable contribution to the solution of the energy crisis of the 21st century. Thermoelectric generators can utilize waste heat from various sources such as combustion engines to generate electrical power and thus increase the energy efficiency of such devices. This form of energy recuperation has various implemented and potential applications in the fields of space flight, traffic, and aviation.<sup>1,2</sup>

The efficiency of such waste heat to electrical energy conversion is governed by the thermoelectric figure of merit  $ZT$ , which is given by basic material properties as

$$ZT = \frac{\sigma S^2}{k} T. \quad (1)$$

A good thermoelectric material thus has high electrical conductivity  $\sigma$ , large Seebeck coefficient  $S$ ,

and low thermal conductivity  $k$ ;  $T$  is the absolute temperature. The identification and especially the optimization of thermoelectric materials require repeated measurement of  $\sigma$ ,  $S$ , and  $k$ , as these three quantities are strongly interdependent and optimization of  $ZT$  cannot be achieved by simple optimization of the individual quantities.<sup>2</sup> This is particularly true for the Seebeck coefficient and the electrical conductivity, which are coupled via the charge carrier concentration of the material: a high charge carrier concentration usually increases  $\sigma$  and decreases  $S$ . For better understanding of measurement results and to reduce the measurement time and sample count, it is highly advantageous to employ a system that can measure  $\sigma$  and  $S$  simultaneously. This is particularly interesting for materials that are unstable under heat treatment, as sequential measurements on the same sample would give misleading results in this case. Although there are some commercially available systems for measurement of  $\sigma$  and  $S$ , we decided to set up a custom-designed system. These are more flexible in measurement routines and measurement data analysis; furthermore, we wanted an apparatus that is applicable up to 1000 K.

(Received July 4, 2012; accepted December 26, 2012;  
published online January 30, 2013)

In this manuscript we first describe the hardware of the setup and its advantages compared with commercially available systems. In the second section we discuss the accuracy of the system and its comparison with other setups. Although strongly needed, there is still no standard material available for Seebeck coefficient measurements above 400 K. We briefly discuss the requirements for such a material and present initial results for  $\text{FeSi}_2$ , which emerges as a possible candidate.

## SETUP

The Seebeck coefficient is the constant of proportionality between the temperature difference  $\Delta T$

across a sample and the voltage  $U$  that arises due to this temperature gradient, i.e.,

$$S = -\frac{U}{\Delta T} = -\frac{U}{T_2 - T_1}, \quad (2)$$

in the limit of a vanishing temperature gradient. For the determination of  $S$ , a temperature gradient is applied across the sample and the resulting voltage is measured. It is highly advantageous to determine  $S$  from a variable temperature gradient, therefore our sample holder is equipped with two gradient heaters (Fig. 1). One heater is sufficient for a variable temperature gradient, but two have the additional advantage that one can vary the gradient in both directions. The heaters are bifilar wound

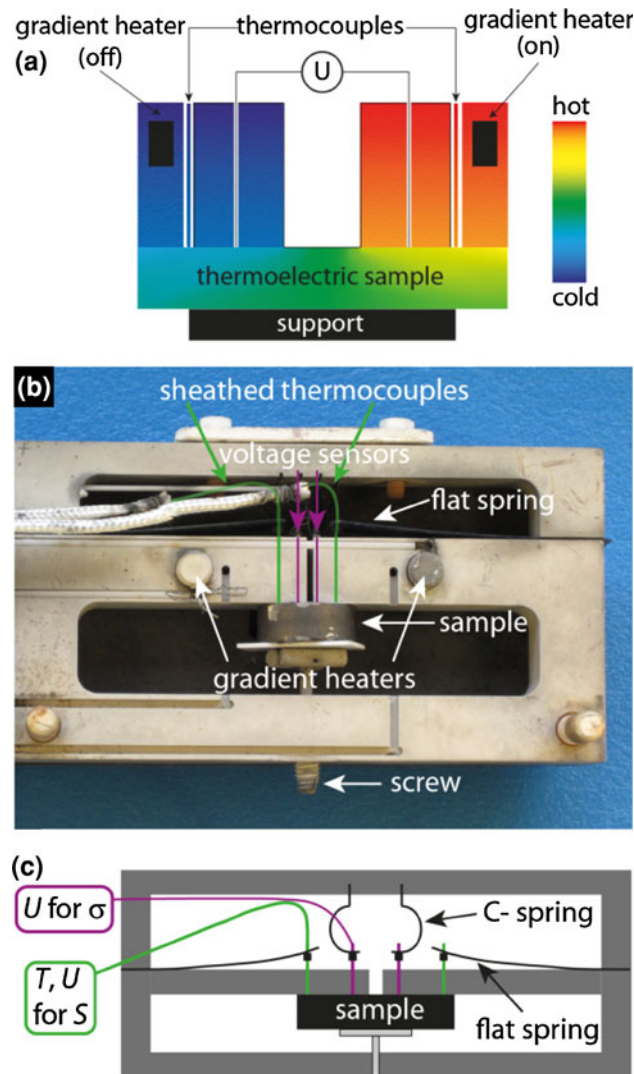


Fig. 1. Sample holder for  $\sigma$  and  $S$  measurement. Two gradient heaters can be used to create a temperature gradient across the sample, which results in Seebeck voltages. The scheme in (a) displays the temperature profile during a measurement of the Seebeck coefficient. The photograph in (b) shows the sample holder with a mounted sample, while the scheme in (c) illustrates the mechanical and electrical connections (only left half shown for clarity). The sheathed thermocouples are used to measure the sample temperatures and the thermoelectric voltages; from these, the Seebeck coefficient  $S$  of the sample under test can be calculated. For the measurement of  $\sigma$ , a current is driven through the sample using the thermocouples for current supply. Additional voltage sensors in line with the thermocouples are used to record the Ohmic voltage drop.

filaments that are heated by supplying electrical power. The temperatures  $T_1$  and  $T_2$  and the thermally induced voltage  $U$  are measured using two sheathed type N thermocouples. Sheathed thermocouples are superior to thermocouples inserted into ceramic tubes (see, e.g., Ref. 3) as they possess some mechanical flexibility that facilitates thermocouple assembly and exchange. The individual thermocouple wires are surrounded by ceramic filling and insulated from each other, while the sheath made from Inconel protects the measuring junction from chemical contamination and provides the mechanical strength that allows the thermocouples to be pressed onto the sample. We employ flat springs made from tungsten-rhenium to press the thermocouples onto the sample. Tungsten-rhenium has large Young's modulus even at elevated temperatures and results in good thermal coupling between the sample and the tips of the thermocouples.<sup>4</sup> This is a prerequisite for accurate measurement of the Seebeck coefficient, since otherwise thermal contact resistances will lead to an erroneous temperature reading and thus an incorrect result for  $S$ . The sample itself is pressed onto the sample holder using a headless screw and a "T"-piece that can be plugged into a hole drilled into the headless screw. The head of the "T"-piece is rotatable and can therefore also be used for samples with nonparallel surfaces.

The electrical conductivity is determined in a four-probe in-line arrangement. The sheath of the thermocouples is used to drive a current through the sample, while two additional probes are used to measure the resulting voltage; from the magnitude of the current, the voltage, the spacing of the tips, and the sample geometry, the electrical conductivity of the sample can be calculated. The voltage probes are made from tungsten carbide and are pressed onto the sample using C-springs made from tungsten-rhenium.

Electrical connection in the high-temperature region (e.g., from platinum wires to the tungsten carbide voltage probes) is made by employing laser spot welding. The sample holder itself is made from Shapal (AlN), a ceramic with good mechanical properties and relatively high thermal conductivity. The components of the sample holder are chosen on the basis of their thermomechanical properties, and while the maximum operating temperature of all parts is well above 1300 K, the maximum operation temperature of the setup is currently restricted to 1000 K as the Young's modulus of the tungsten-rhenium springs reduces significantly above 1050 K.

The sample holder is covered on both sides by graphite semicylinders that are attached to the sample holder using ceramic screws. The semicylinders homogenize the thermal environment and serve as radiation shields. The sample holder is connected to a vacuum flange by a molybdenum rod; the flange covers a quartz glass tube which

contains the sample holder. The glass tube is connected to a vacuum pump and can be operated under vacuum ( $p \approx 10^{-5}$  mbar) or inert gas atmosphere. The glass tube plus sample holder is inserted into a tube furnace (Thermconcept) that is used to regulate the ambient temperature. The furnace, gradient heater power supply, as well as measurement electronics (Agilent 33210A, Keithley 2700 + switch card 7700) are connected to a PC via a GPIB interface and are operated using a custom-made Visual Basic program. There have been several reports on setups for the measurement of  $S$  and  $\sigma$ .<sup>5–11</sup> Compared with these, our measurement system distinguishes itself by having large flexibility in sample dimensions (10 mm < length < 30 mm, 0.1 mm < thickness < 8 mm), very low maintenance requirements, and very easy sample exchange: since all electrical connections are made with pressure contacts, exchanging the sample requires only mounting the sample on the T-piece and fastening the screw. The system accommodates parallelepiped and cylindrical samples. The latter option is crucial, as this is the typical geometry for thermal conductivity measurements with the frequently employed laser flash method.

We now briefly describe the measurement procedure for  $\sigma$  and  $S$ . First, the desired temperature is set in the furnace and stabilized. Then, an alternating current  $I$  is passed through the sheath of the thermocouples and the resulting voltage  $U$  between the tungsten carbide probes is recorded. The sample conductivity is then calculated from

$$\sigma = \frac{1}{2\pi s UC}, \quad (3)$$

where  $s$  is the spacing between the tips and  $C$  is a geometrical correction factor. This correction factor accounts for the finite size of the sample, its geometry, and the spacing between the tips. For typical geometries such as bar-shaped or cylindrical samples, correction factors have been reported in the literature. We have employed the values reported in Refs. 12–15.

The Seebeck coefficient can in principle be determined from

$$S = -\frac{U_A}{T_2 - T_1} + S_A, \quad (4)$$

where  $U_A$  is the voltage measured across the two thermocouple wires of type A (in our case, A: Nisil, B: Nicrosil) and  $S_A$  is the Seebeck coefficient of the wire material; the equivalent equation holds true for  $U_B$ . However, determination of  $S$  from a single temperature–voltage pair can be highly inaccurate due to spurious thermal voltages within the measurement system and imperfections of the employed thermocouples. To record the voltages and temperatures for a number of data points, we first run heater 1 for a short time, typical 60 s. A temperature difference arises, see Fig. 2.

The heater is switched off, and the system relaxes; during this time,  $T_1$ ,  $T_2$ ,  $U_A$ , and  $U_B$  are recorded and used for later analysis. The step is repeated for heater 2. Instead of using single voltage–temperature pairs we can now employ the slope of  $U_A$  versus  $U_B$  to calculate  $S$ .

The two recorded voltages  $U_A$  and  $U_B$  are given by

$$U_A = -(S - S_A)\Delta T; \quad U_B = -(S - S_B)\Delta T, \quad (5)$$

which can be rewritten as

$$\frac{\partial U_A}{\partial \Delta T} = -S + S_A; \quad \frac{\partial U_B}{\partial \Delta T} = -S + S_B. \quad (6)$$

Combining these two equations to replace  $\Delta T$  yields after some math

$$S(\bar{T}) = \frac{S_{TC}(\bar{T})}{1 - \frac{\partial U_B}{\partial U_A}} + S_A(\bar{T}), \quad (7)$$

with the mean temperature  $\bar{T}$  and  $S_{TC} = S_B - S_A$ , where  $S_{TC}$  is the Seebeck coefficient of the thermocouple as tabulated and  $S_A$  is the wire with the more negative Seebeck coefficient. Employing Eq. (7) instead of Eq. (4) is highly advantageous for several reasons. Firstly, spurious thermal offset voltages from the system are cancelled, since only the slope and no absolute values are used. In contrast to the equation used in Ref. 5, Eq. (7) does not require the thermal offset voltages of  $U_A$  and  $U_B$  to be the same with respect to  $\Delta T$ ; the offsets just have to be constant. Secondly, the equation requires no direct temperature measurements, which tend to be less accurate than voltage measurements. Temperatures are only required for the calculation of the mean temperature  $\bar{T}$ , where accuracy is less important.

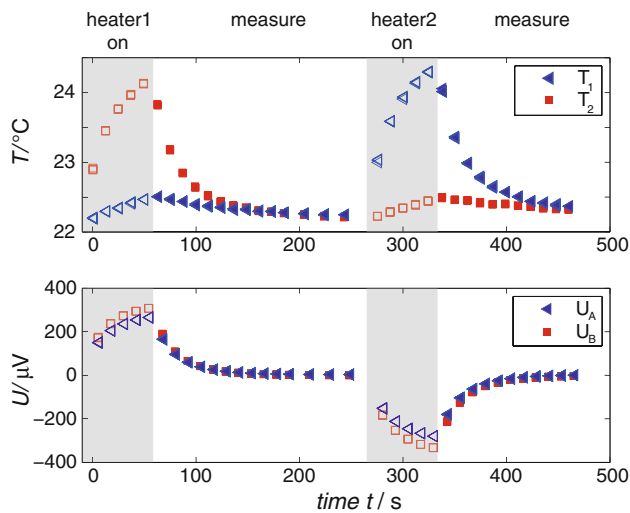


Fig. 2. Measurement routine for determination of the Seebeck coefficient. First, heater 1 is switched on and a temperature gradient arises. After a short time, the heater is switched off and the system relaxes; finally, the step is repeated with heater 2. Temperatures and voltages are recorded for the complete measurement cycle, but only the data acquired during relaxation are used for calculation of  $S$ .

Finally by taking the slope from a large number of data points, statistical errors in the voltage readings of the individual points are of less significance, as they are averaged. A representative plot of  $U_B$  versus  $U_A$  is shown in Fig. 3. Also given in the figure is the linear correlation coefficient  $R$  of the linear fit, which can be used to judge the quality of the measurement and to check for errors.

### MEASUREMENT UNCERTAINTY ANALYSIS AND COMPARISON WITH REFERENCE DATA

We begin with a discussion of the uncertainties of the  $\sigma$  measurement.  $\sigma$  is calculated from Eq. (3), and thus uncertainties can stem from noisy voltage readings affecting  $R$  or from geometrical uncertainties of the sample or probe spacing, affecting  $s$  or the geometrical correction factor  $C$ . The voltage probes are rigid and have an allowance for clearance of less than  $50 \mu\text{m}$ , and their separation can be measured using optical microscopy with high accuracy. The thermocouples have a larger allowance for clearance and show a variation of  $\approx 100 \mu\text{m}$ , which can lead to an uncertainty in  $\sigma$  of some percent. Additional uncertainties arise from incorrect measurements of the sample dimensions which affect the calculation of  $C$  and improper positioning of the sample with respect to the tips. Most calculations of  $C$  either assume a sample that is symmetrical with respect to the tips<sup>12</sup> or a known distance from the tips to the sample edge.<sup>14</sup> Nevertheless, comparison with a different setup in-house that determines the electrical conductivity based on the van der Pauw method<sup>16</sup> shows agreement better than 5% and typically better than 3%.

The error of environment temperature in the  $\sigma$  and  $S$  measurement is governed by the accuracy of the thermocouples, which are class 1 in our case. The Seebeck coefficient measurement is necessarily obtained from a temperature interval; in our case,

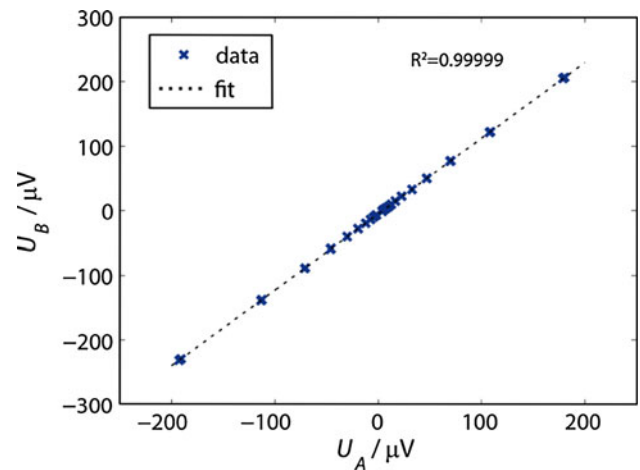


Fig. 3. Plot of  $U_B$  versus  $U_A$ . The slope of  $U_B$  versus  $U_A$  is used to determine the Seebeck coefficient, see Eq. (7). The linear fit is excellent, as can be deduced from the correlation coefficient  $R$ .

the temperature  $S(\bar{T})$  is taken as the average over all recorded temperatures in one measurement cycle, see Fig. 2. The temperature interval over which the measurement is taken is usually  $<2$  K, which is small compared with the typical spacing of the temperature points where measurements are taken.

The uncertainties of the Seebeck coefficient measurement itself stem from several sources. First, there are inaccuracies of the voltage readings used to determine  $S$ . Since the recorded voltages are usually small ( $250 \mu\text{V} < U_A, U_B < 2 \mu\text{V}$ ), the noise can have some effect on the measurement result. Another possible source of uncertainty is the interpolation of the recorded voltages with respect to time, which is necessary as Eq. (7) (and also Eq. 4) requires the respective quantities to be recorded simultaneously. While Eq. (7) is not affected by thermal offset voltages (like  $U_A = 0$  for  $U_B = 0$ ), it nevertheless requires an offset which is constant over the measurement time. A changing offset voltage will affect the result for  $S$  but can be identified by a correlation coefficient not close to unity, see Fig. 3.

The potentially most severe uncertainty stems from thermal contact resistances between the sample, the thermocouples, and the part of the sample holder pressed onto the sample. These can cause a discrepancy between the Seebeck voltage reading and the temperature reading and therefore an incorrectly determined Seebeck coefficient.<sup>8</sup> Equation (7), which is used in our setup, does not require the temperatures to determine  $S$ , but the voltages  $U_A = 0$  and  $U_B = 0$  are affected in the same manner as the temperatures by thermal contact resistances.

The statistical errors due to electrical noise, the effect of the data interpolation, as well as a varying offset can be estimated by variation of the measurement parameters and are found to cause an error of  $<4\%$  for the presented setup. The effect of the thermal contact resistances depends on various physical parameters (sample hardness, surface roughness, temperature, pressure of the sample against the sample holder, pressure of thermocouples against sample, pressure and type of surrounding atmosphere, etc.) that are partially poorly accessible and controllable in the experiment. To get an estimation for the absolute accuracy of the developed setup, it is therefore necessary to compare the measurement results with known references or the results of other setups.

To date, there is no standard reference material for the Seebeck coefficient above 400 K, although research in this direction is underway.<sup>17,18</sup> We have therefore used a twofold strategy to proof the accuracy of our setup, labeled HTS $\sigma$  in the following. First we used a different custom-built setup (“CTEM”) to measure the recently published NIST standard reference material for low-temperature Seebeck coefficient measurements (SRM 3451).<sup>19</sup> The results for the NIST reference material are

presented in Fig. 4 and show excellent agreement with the measured data. We cannot measure the NIST standard reference material in the presented HTS $\sigma$  setup, as the length of the SRM 3451 sample is only 8 mm, and thus too small.

After proofing the accuracy of the CTEM, in a second step we compared the measurement results between CTEM and HTS $\sigma$ . Results for a CoSb<sub>3</sub> skutterudite sample are plotted in Fig. 5 and show very good agreement between CTEM and HTS $\sigma$  results up to  $\approx 550$  K, which is the current maximum operation temperature for the CTEM setup.

Apart from this indirect comparison with the NIST reference material, we checked the accuracy of the presented HTS $\sigma$  setup by comparative measurements of two further samples in different setups. Traditionally, pure metals such as Ni are often used as reference materials.<sup>4,10</sup> Here, we used two commercially available Ni-based alloys as reference materials, because their material properties are closer to those of actual thermoelectric materials. The results shown in Fig. 6 are related to the first sample with approximate composition Cu<sub>45</sub>Ni<sub>55</sub> and dimensions 17 mm  $\times$  10 mm  $\times$  1.0 mm (Silverin 404; Auerhammer Metallwerk GmbH). The measurements were performed with CTEM, HTS $\sigma$ , and an apparatus situated at the Physikalisch-Technische Bundesanstalt (PTB), the German Metrology Institute. Their system<sup>20</sup> is an improved version of the apparatus presented in Ref. 5. It can be seen that all three systems show good agreement over the whole temperature range, with maximal deviation of less than 4%.

The results for the second sample (Cu<sub>54</sub>Ni<sub>44</sub>Mn<sub>1</sub>, 24 mm  $\times$  11 mm  $\times$  0.3 mm, ISOTAN; Isabelenhütte Heusler GmbH & Co. KG, Germany) are shown in Fig. 7 together with the measurement results for the electrical conductivity. The magnitude of the sample’s Seebeck coefficient is around

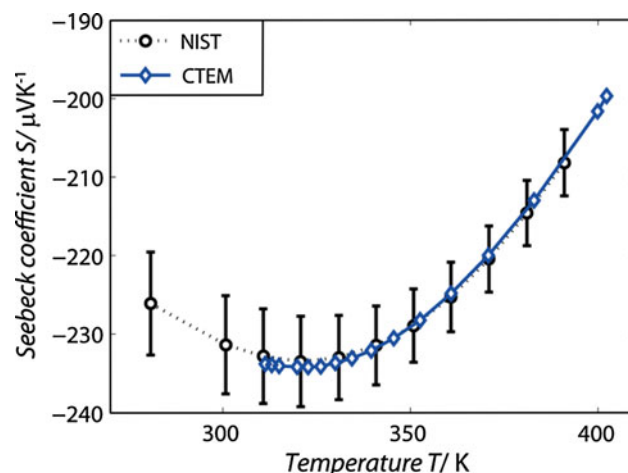


Fig. 4. Comparison of the Seebeck coefficient measured from NIST SRM 3451 using the custom-built system CTEM (blue). The black points indicate the published data from NIST, while the error bars indicate the stated measurement uncertainty. The black and blue curve show excellent agreement with maximal deviations of 1%.

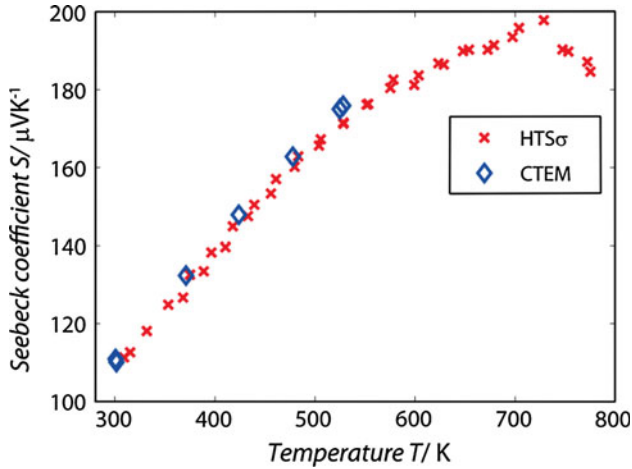


Fig. 5. Comparison of the measurement results for the Seebeck coefficient measured by the CTEM and HTS $\sigma$ . A hot-pressed skutterudite was used as the sample. The two datasets show good agreement.

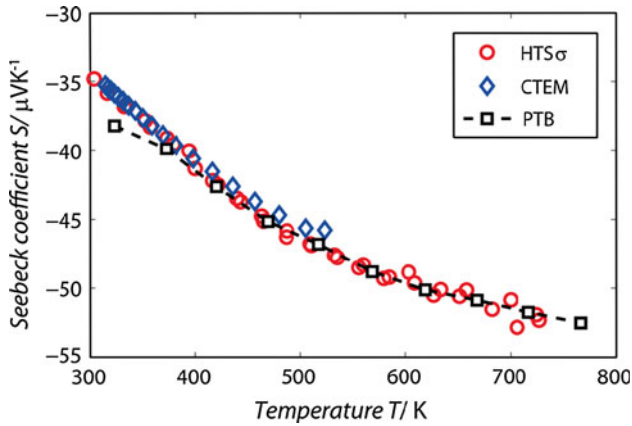


Fig. 6. Comparison of Seebeck coefficient of  $\text{Cu}_{45}\text{Ni}_{55}$  measured using three different setups: HTS $\sigma$  and CTEM in-house, as well as an apparatus from the PTB. The agreement between all three datasets is very good.

$-37 \mu\text{V/K}$  at room temperature and increases with temperature. The datasets for both samples compare very well and show a maximum deviation of 4% from each other. The electrical conductivity of the second sample shows weak temperature dependence. This is not surprising as the alloy has a composition similar to constantan.

All presented measurements were taken in helium atmosphere at pressure of  $p \approx 1$  bar. Compared with vacuum, a He atmosphere decreases the thermal contact resistances between the sample, thermocouple, and sample holder and can improve the measurement accuracy;<sup>4</sup> outgassing from the samples is also reduced. From the discussion of the measurement errors, the comparison with reference data, and with results from different setups, we can deduce that the Seebeck coefficient can be measured with accuracy of around 5% in the temperature regime from 300 K to 1000 K.

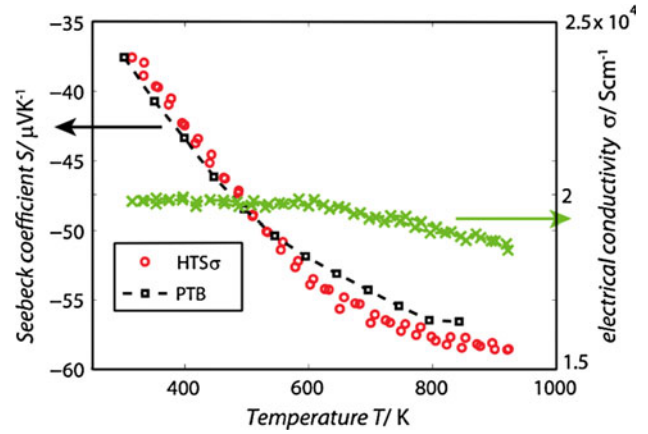


Fig. 7. Seebeck coefficient and electrical conductivity of  $\text{Cu}_{54}\text{Ni}_{44}\text{Mn}_1$ . Also shown is the comparative measurement of the Seebeck coefficient at PTB, again confirming the measurement data from the HTS $\sigma$  setup.

## TOWARDS A HIGH-TEMPERATURE SEEBECK STANDARD

To realize various thermoelectric applications, materials identification and optimization are required. This process includes systematic studies of fabrication parameter variation, and accurate measurements of thermoelectric properties are indispensable for evaluation of these studies and thus for efficient material optimization. This is particularly true for the Seebeck coefficient, which enters the thermoelectric figure of merit squared and thus governs the conversion efficiency of materials to a large extent. For trustworthy and meaningful measurements, comparison of the employed setup with references is necessary. Such a standard material has recently been presented for the low-temperature regime.<sup>19</sup> For the high-temperature regime above 400 K, where many attractive applications exist, no standard material exists yet. This hinders comparison between different thermoelectric measurement setups and slows the material development process. A possible high-temperature standard material has to fulfill a number of requirements: it must be mechanically and thermally stable in the required temperature regime, its fabrication must be reproducible, and the sample properties must be spatially homogeneous and typical of thermoelectric materials; the material should furthermore be chemically inert. An inexpensive material that is nontoxic and fulfills environmental regulations is advantageous, as this simplifies handling and facilitates the establishment of the standard.

Among the many materials under investigation,  $\beta\text{-FeSi}_2$  is one possible candidate. We have employed the presented setup for evaluation of the Seebeck coefficient of several  $\text{FeSi}_2$  samples. These were produced from a gas-atomized powder with nominal composition  $\text{Fe}_{0.95}\text{Co}_{0.05}\text{Si}_2$ . Compaction was achieved by a direct-current-assisted short-term sintering process at 1173 K for 30 min at heating rate of 60 K/s and mechanical load of 50 MPa. This

compaction was followed by 24 h annealing at approximately 1100 K to form the desired semi-conducting  $\beta$ -FeSi<sub>2</sub>.<sup>21</sup> The detailed fabrication parameters will be the subject of a future publication; here, we focus on the suitability of this material as a high-temperature Seebeck reference material.

The spatial homogeneity of samples can be investigated using a potential Seebeck micro-probe.<sup>22</sup> The results of the local Seebeck coefficient of one sample are presented in Fig. 8. The sample shows a very narrow distribution of the Seebeck coefficient with full-width at half-maximum of 2.5  $\mu\text{V/K}$ , which equals 1.7% of the statistical mean value.

We have investigated the thermal stability of FeSi<sub>2</sub> samples by employing the presented setup. We therefore exposed one of the samples to several thermal cycles up to 1000 K as shown in Fig. 9a. The corresponding results for the Seebeck coefficient are presented in Fig. 9b. For clarity, polynomial fits to the measurement data are plotted together with the raw measurement results. The maximum deviation of the polynomial fits from each other is  $\approx 2\%$  of the absolute value and shows no systematic drift with temperature. We can therefore deduce that the prepared FeSi<sub>2</sub> is thermally stable up to 1000 K, which is one crucial requirement for a high-temperature standard material.

Another important criterion for a reference material is the reproducibility of the samples. Figure 10 compares the measurement results of the first sample with a further sample that is not from the same batch but fabricated under the same conditions. The measurement results are very close to each other, as exemplified by the polynomial fits that are plotted for clarity. These fits differ by less than 2% over the whole temperature range, which is less than the measurement uncertainty. Comparison

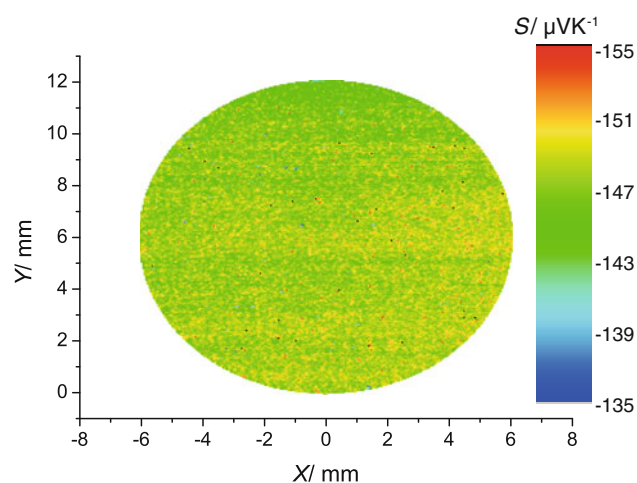


Fig. 8. Spatial scan of the Seebeck coefficient of a  $\beta$ -FeSi<sub>2</sub> sample. It can be seen that the sample is very homogeneous; the full-width at half-maximum of the Seebeck coefficient distribution is only 1.7% of the mean value.

of two samples is clearly not sufficient to prove reproducibility, but it indicates that the fabrication process is well understood and that consistent production of samples is feasible.

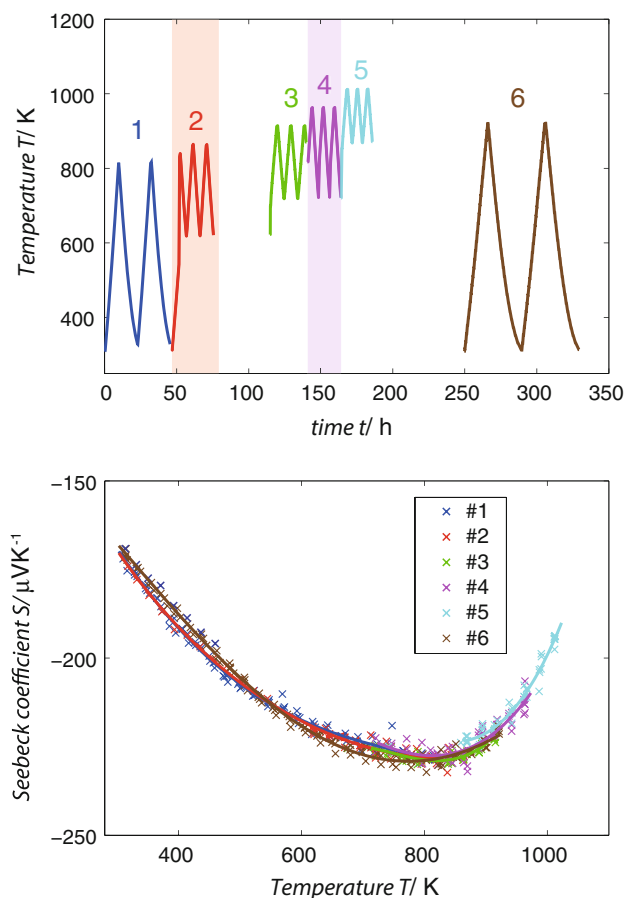


Fig. 9. (a) Thermal cycling program and (b) corresponding results for the Seebeck coefficient. In (b) the corresponding raw measurement data are shown together with polynomial fits for better clarity. No significant change of Seebeck coefficient can be seen after repeated thermal cycling of the sample, partially above 1000 K.

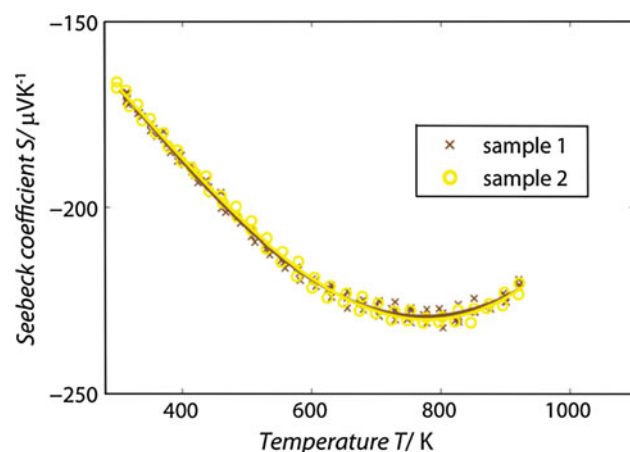


Fig. 10. Comparison of the Seebeck coefficient of two FeSi<sub>2</sub> samples. The two samples show very similar values, indicating reproducible sample fabrication.

It can be concluded that FeSi<sub>2</sub> fulfills several requirements of a high-temperature Seebeck standard: good spatial homogeneity over relatively large sample size, thermoelectric properties in a typical range, mechanical stability, low price, nontoxicity, as well as thermal stability of the Seebeck coefficient; reproducible fabrication is indicated.

Despite the shown encouraging results for FeSi<sub>2</sub>, further experiments are necessary to decide whether the material can be used as a high-temperature standard material. These include further comparisons between different samples, long-time thermal cycling experiments, as well as round-robin measurements.

## CONCLUSIONS

We have presented a setup for concurrent measurement of the electrical conductivity and Seebeck coefficient. The setup features a large operating temperature regime (300 K to 1000 K), flexibility in sample geometry, as well as easy and fast sample exchange. We have presented details on the hardware of the system as well as the data analysis employed for determination of the Seebeck coefficient. To verify the accuracy of the presented setup, we have compared measurement results on the NIST low-temperature standard sample as well as other materials in different setups in two different laboratories and showed very good agreement. The system was employed in the search for a possible high-temperature standard reference material for the Seebeck coefficient. We have investigated the thermoelectric properties of  $\beta$ -FeSi<sub>2</sub> and could show good spatial homogeneity as well as thermal stability for the Seebeck coefficient, which makes this material a suitable choice as a future reference material. A readily available Seebeck standard will increase the trustworthiness of measurement results from thermoelectric materials and thus facilitate progress in material optimization.

## ACKNOWLEDGEMENTS

H. Kolb is acknowledged for the comparative electrical conductivity measurements. Financial support from the BMBF Projects INTEG (03X3555A) as well as TEST (03X3550B) is gratefully acknowledged.

## REFERENCES

1. L.E. Bell, *Science* 321, 1457 (2008).
2. G.S. Snyder and E.S. Toberer, *Nat. Mater.* 7, 105 (2008).
3. S. Iwanaga, E.S. Toberer, A. LaLonde, and G.J. Snyder, *Rev. Sci. Instrum.* 82, (2011).
4. A.T. Burkov, A. Heinrich, P.P. Konstantinov, T. Nakama, and K. Yagasaki, *Meas. Sci. Technol.* 12, (2001).
5. O. Boffoue, A. Jacquot, A. Dauscher, B. Lenoir, and M. Stölzer, *Rev. Sci. Instrum.* 76, 053907, (2005).
6. C. Byl, D. Bérardan, and N. Dragoe, *Meas. Sci. Technol.* 23, 035603 (2012).
7. J. Martin, *Rev. Sci. Instrum.* 83, 065101 (2012).
8. P.H. Michael, E. Flage-Larsen, O.B. Karlsen, and T.G. Finstad, *Rev. Sci. Instrum.* 83, 025101 (2012).
9. V. Ponnambalam, S. Lindsey, N.S. Hickman, and T.M. Tritt, *Rev. Sci. Instrum.* 77, 073904 (2006).
10. J. de Boor and V. Schmidt, *Adv. Mater.* 22, 4303 (2010).
11. J. de Boor and V. Schmidt, *Appl. Phys. Lett.* 99, 022102 (2011).
12. E. Hansen, *Appl. Sci. Res.* 8, 93 (1960).
13. A. Uhlir, *Bell Labs Tech. J* 105, (1955).
14. L. Valdes, *P. IRE* 42, 420 (1954).
15. F. Smits, *Bell Labs Tech. J* 37, 711 (1958).
16. L.J. van der Pauw, *Philips Res. Rep.* 13, 1 (1958).
17. N. W. Wong-Ng, NIST, personal communication.
18. P. Ziolkowski, P. Blaschkewitz, G. Karpinski, C. Stiewe, and E. Müller, *European Conference on Thermoelectrics: ECT*, (2011).
19. N.D. Lowhorn, W. Wong-Ng, Z.-Q. Lu, J. Martin, M.L. Green, J.E. Bonevich, E.L. Thomas, N.R. Dille, and J. Sharp, *J. Mater. Res.* 26, 1983 (2011).
20. E. Lenz, S. Haupt, F. Edler, P. Ziolkowski and H. F. Pernau, *Phys. Stat. Sol.*, 12, 2432 (2012). doi:10.1002/pssc.201200305.
21. Z. He, D. Platzek, C. Stiewe, H. Chen, G. Karpinski, and E. Mueller, *J. Alloys Compd.* 438, 303 (2007).
22. P. Ziolkowski, G. Karpinski, D. Platzek, C. Stiewe, and E. Mueller *ICT 2006, 25th Int. Conf. Thermoelect.* (Piscataway, NJ: IEEE, 2006), p. 684.